isolator at all. Examination of Figs. 3(b), (c), and (d) reveals that a TE_{10} signal incident from the right at port 2 exits port 1 in the TE_{01}-mode, is reflected, exits port 2 in the same mode, is again reflected, and ultimately exits port 1 unimpeded in the TE_{10}-mode.

III. Discussion

Our motivation for examining the inherent noise of isolators came from the fact that we wished to use them in a noise measurement system at 94 GHz, with the goal of detecting the quantum noise of devices at 2 K. Some details of the measurement system envisioned are given in a companion paper [2]. It became obvious that the Nyquist noise due to the termination of port 3 of a circulator used as an isolator would be intolerable for our purpose. Naively, we thought that a Faraday rotation isolator embodied in the form of Fig. 2 might behave differently. We then undertook the analysis given above and discovered, much to our surprise, that it behaved exactly as a terminated circulator. Only then did we discover Siegman's incontrovertible and beautifully simple proof of that fact.

IV. Conclusion

To achieve isolation between its input and output ports, an isolator *must* include at least one resistive source of Nyquist noise. That noise emanates from its input port. Siegman's thermodynamic proof cannot be denied.

Acknowledgment

This work was supported by National Science Foundation Grant ECS-8007623. A. van der Ziel suggested to the author that the inherent noise of an isolator required exploration.

References

[1] A. E. Siegman, "Thermal noise in microwave systems, part I," *Microwave J.*, vol. 4, pp. 81–90, Mar. 1961.

[2] A. D. Sutherland and A. van der Ziel, "Some pitfalls in millimeter-wave noise measurements utilizing a cross-correlation receiver," *IEEE Trans. Microwave Theory Tech.*, this issue, 715–718.

The Exact Noise Figure of Amplifiers with Parallel Feedback and Lossy Matching Circuits

KARL B. NICLAS, SENIOR MEMBER, IEEE

***Abstract*—Exact formulas for the noise parameters and noise figure of amplifiers with parallel feedback and lossy input and output matching circuits are derived. The formulas which take into account the thermal agitation of all circuit elements are applicable to feedback and lossy match amplifiers, as well as amplifiers that employ both principles simultaneously.**

I. Introduction

Recent developments in the design of single-ended GaAs MESFET amplifiers have focused on two principles, parallel feedback and lossy matching [1]–[3]. Either principle has enormous bandwidth potential, ranging from a few megahertz all the way into *Ku*-band. Investigation of the noise in microwave amplifiers with parallel feedback have proven their feasibility for low-noise amplification [4]. When comparing noise figures of feedback amplifiers with those of equivalent amplifiers that use lossy matching circuits, the latter exhibit both, higher theoretical and measured values [5]. However, the lossy match amplifier has the advantage that dc-biasing can be accomplished without seriously reducing the amplifier's bandwidth potential in the megahertz region. A compromise in electrical performance may be found in the combination of both principles.

Employing parallel feedback and/or lossy matching for low-noise applications requires a qualitative study of the influence of all circuit components on the amplifier's noise figure. Several papers on the noise figure of amplifiers with parallel feedback have been published over the last eight years [6]–[9]. However, except for [9] the published results do not take into account the inherent noise sources of the transforming two-ports and therefore cannot be applied to amplifiers that make use of resistive feedback and/or lossy matching networks. This paper develops the exact formulas for the equivalent noise parameters and the noise figure of an amplifier that simultaneously uses parallel feedback and lossy matching while allowing for the thermal noise agitation of all circuit elements. Due to the fact that the results presented here differ from those obtained by applying the formulas presented in [9], a step-by-step account of the deriviations is given in the Appendix.

II. Noise Figure and Equivalent Noise Parameters

To study the noise of a two-port with internal noise sources, it is replaced by a noise-free two-port preceded by a simple circuit containing its equivalent noise parameters [10]. The latter consists of the equivalent noise resistance R_n, the equivalent noise conductance G_n, and the correlation admittance $Y_{\text{cor}} = G_{\text{cor}} + jB_{\text{cor}}$. The parameters R_n, G_n, and Y_{cor} can be calculated in case the noise figure for optimum noise matching $F_{\min}$, the corresponding signal source admittance $Y_{s\min} = G_{s\min} + jB_{s\min}$, and one other noise figure F and its corresponding signal source admittance $Y_s = G_s + jB_s$, preferably $Y_s = Z_0^{-1}$, are known.

The noise figure of a two-port can be expressed by the well-known formulas [10], [11]

$$F = F_{\min} + \frac{R_n}{G_s}(G_s - G_{s\min})^2 + \frac{R_n}{G_s}(B_s - B_{s\min})^2 \qquad (1)$$

with

$$F_{\min} = 1 + 2\left[R_n G_{\text{cor}} + \sqrt{R_n G_n + (R_n G_{\text{cor}})^2}\right]. \qquad (2)$$

The circuit whose overall noise figure we want to determine is shown in Fig. 1(a). It consists of a noisy two-port at temperature T embedded in a π-shaped network of three admittances Y_G, Y_{FB}, and Y_D. They contain the conductances G_G, G_{FB}, and G_D which inject noise into the overall two-port of Fig. 1(a) and thereby contribute to the noise figure of the overall network.

In Fig. 1(b) all internal noise sources of the embedded two-port and the surrounding admittances have been extracted and are represented as external noise voltages (v_1, v_{FB}) and noise currents (i_1, i_G, i_D). This step puts all circuit elements and the embedded two-port at $T = 0$ K.

The network of Fig. 1(b) will now be used to determine the noise parameters as shown in Fig. 1(c). In doing so, we follow the procedure as outlined in [4] based on [10]. The admittance matrix of the noiseless network of Fig. 1(c) representing the signal voltages and currents takes the form

Manuscript received October 12, 1981; revised December 15, 1981.

The author is with the Devices Group, Watkins-Johnson Company, 3333 Hillview Ave., Stanford Industrial Park, Palo Alto, CA 94304.

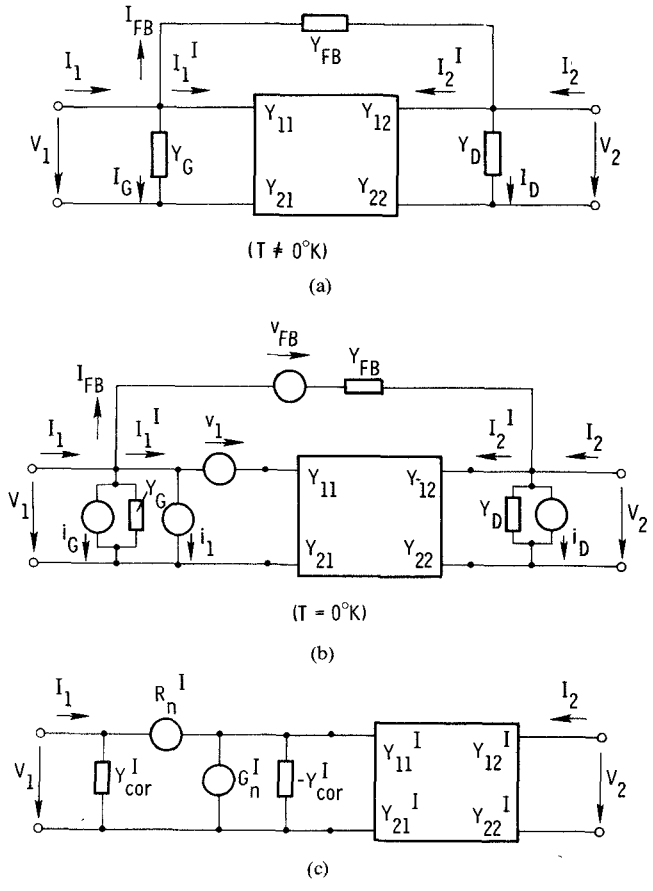

Fig. 1. (a) Amplifier with parallel feedback and lossy matching circuits (internal noise sources). (b) Equivalent circuit of (a) with external noise sources v_1, v_{FB}, i_1, i_G, and i_D. (c) Equivalent circuit of (a) with uncorrelated noise sources R_n^I and G_n^I at $T=T_0$ and correlation admittance Y_{cor}^I at $T=0$ K.

$$\boldsymbol{Y}=\begin{vmatrix} Y_{11}^I & Y_{12}^I \\ Y_{21}^I & Y_{22}^I \end{vmatrix}=\begin{vmatrix} (Y_{11}+Y_G+Y_{FB}) & (Y_{12}-Y_{FB}) \\ (Y_{21}-Y_{FB}) & (Y_{22}+Y_D+Y_{FB}) \end{vmatrix}. \quad (3)$$

The expressions for the equivalent noise parameters which were derived in the Appendix, are

$$R_n^I=\frac{\overline{|v_1^I|^2}}{4KT_0\Delta f}=\frac{1}{|Y_{21}-Y_{FB}|^2}\left[|Y_{21}|^2R_n+|Y_{FB}|^2R_{FB}+G_D\right] \quad (4a)$$

$$G_n^I=\frac{\overline{|i_n^I|^2}}{4KT_0\Delta f}=\frac{1}{4KT_0\Delta f}\left[\overline{|i_1^I|^2}-\frac{\overline{|i_1^I(v_1^I)^*|^2}}{\overline{|v_1^I|^2}}\right]$$

$$=G_n+G_G+|Y_{21}+Y_{11}-Y_{cor}|^2\frac{|Y_{FB}|^2R_{FB}R_n}{|Y_{21}|^2R_n+|Y_{FB}|^2R_{FB}+G_D}$$

$$+\frac{|Y_{11}-Y_{cor}|^2R_n+|Y_{FB}|^2R_{FB}}{|Y_{21}|^2R_n+|Y_{FB}|^2R_{FB}+G_D}G_D \quad (4b)$$

$$Y_{cor}^I=\frac{\overline{i_1^I(v_1^I)^*}}{\overline{|v_1^I|^2}}$$

$$=Y_G+Y_{cor}+(Y_{21}+Y_{11}-Y_{cor})\frac{Y_{21}^*Y_{FB}R_n+|Y_{FB}|^2R_{FB}}{|Y_{21}|^2R_n+|Y_{FB}|^2R_{FB}+G_D}$$

$$+(Y_{11}+Y_{FB}-Y_{cor})\frac{G_D}{|Y_{21}|^2R_n+|Y_{FB}|^2R_{FB}+G_D}. \quad (4c)$$

TABLE I
COMPARISON OF EXACT AND APPROXIMATED NOISE PARAMETERS

Frequency (GHz)	2	4	6	8	Dimension	Formula
R_n	20.8	32.3	53.1	122.0	Ω	
G_n	0.16	3.7	13.1	20.9	mS	
G_{cor}	5.9	-0.9	-13.9	-23.0	mS	
B_{cor}	3.7	11.1	13.0	7.3	mS	
$\|Y_{21}\|^2 R_n$	68	172	602	2254	mS	(6a)
$\|Y_{FB}\|^2 R_{FB}+G_D$	5.3	5.3	5.3	5.3	mS	(6a)
$\|Y_{21}+Y_{11}-Y_{cor}\|^2$	2.57	5.41	11.47	20.56	10^{-3} S^2	(6b)
$\|Y_{11}-Y_{cor}\|^2$	0.046	0.017	0.407	2.86	10^{-3} S^2	(6b)
R_n^I	22.2	33.8	54.0	121.5	Ω	(4a)
R_n^I	24.0	34.8	54.5	121.6	Ω	(7a)
G_n^I	5.7	9.8	19.1	27.2	mS	(4b)
G_n^I	5.7	9.3	17.9	24.6	mS	(7b)
G_{cor}^I	12.1	5.1	-7.9	-16.5	mS	(4c)
G_{cor}^I	12.6	6.0	-6.4	-15.7	mS	(7c)
F_{min}^I	3.9	4.1	3.7	3.8	dB	(2) & (4)
F_{min}^I	4.1	4.2	3.8	3.7	dB	(2) & (7)
Gain	7.7	7.9	8.0	7.2	dB	

Even though the above formulas are fairly complex, they can be significantly reduced once the magnitudes of $|Y_{21}|^2R_n$, $|Y_{FB}|^2R_{FB}$, and G_D are compared and smaller terms are dropped. In many practical cases the influence of G_D can be entirely neglected resulting in

$$R_n^I=\frac{1}{|Y_{21}-Y_{FB}|^2}\left[|Y_{21}|^2R_n+|Y_{FB}|^2R_{FB}\right] \quad (5a)$$

$$G_n^I=G_n+G_G+|Y_{21}+Y_{11}-Y_{cor}|^2\frac{|Y_{FB}|^2R_{FB}R_n}{|Y_{21}|^2R_n+|Y_{FB}|^2R_{FB}} \quad (5b)$$

$$Y_{cor}^I=Y_G+Y_{cor}+(Y_{21}+Y_{11}-Y_{cor})\frac{Y_{21}^*Y_{FB}R_n+|Y_{FB}|^2R_{FB}}{|Y_{21}|^2R_n+|Y_{FB}|^2R_{FB}}. \quad (5c)$$

If the conditions

$$|Y_{21}|^2R_n\gg\left(|Y_{FB}|^2R_{FB}+G_D\right) \quad (6a)$$

and

$$|Y_{21}+Y_{11}-Y_{cor}|^2\gg|Y_{11}-Y_{cor}|^2 \quad (6b)$$

are satisfied, which is the case in many practical applications, the equivalent noise parameters (4) can be simplified to

$$R_n^I=\left|\frac{Y_{21}}{Y_{21}-Y_{FB}}\right|^2R_n \quad (7a)$$

$$G_n^I=G_n+G_G+|Y_{21}+Y_{11}-Y_{cor}|^2\left|\frac{Y_{FB}}{Y_{21}}\right|^2R_{FB} \quad (7b)$$

$$Y_{cor}^I=Y_G+Y_{cor}+Y_{FB}+(Y_{11}-Y_{cor})\frac{Y_{FB}}{Y_{21}}. \quad (7c)$$

In Table I we compare the noise parameters and noise figures

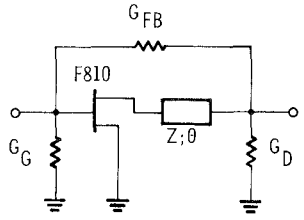

Fig 2 Circuit diagram of an amplifier with parallel feedback and lossy matching circuits ($G_G = 4$ mS, $G_D = 3.3$ mS, $G_{FB} = 2$ mS, $Z = 90\ \Omega$, $\theta = 45°$ at 8 GHz)

of a simple 2–8-GHz amplifier that employs both parallel feedback and lossy matching. The module's circuit diagram and its elements are shown in Fig. 2. The comparison demonstrates that the conditions of (6) are satisfied for this example of a realizable amplifier and also shows that exact (4) and approximated (7) noise figures are within 0.2 dB of each other.

For the lossy match amplifier, i.e., $Y_{FB} = 0$, the equivalent noise parameters (4) take the relatively simple form

$$R_n^{\mathrm{I}} = R_n + \frac{G_D}{|Y_{21}|^2} \tag{8a}$$

$$G_n^{\mathrm{I}} = G_n + G_G + |Y_{11} - Y_{\mathrm{cor}}|^2 \frac{G_D R_n}{|Y_{21}|^2 R_n + G_D} \tag{8b}$$

$$Y_{\mathrm{cor}}^{\mathrm{I}} = Y_{\mathrm{cor}} + Y_G + (Y_{11} - Y_{\mathrm{cor}}) \frac{G_D}{|Y_{21}|^2 R_n + G_D}. \tag{8c}$$

The formulas of the equivalent noise parameters for the amplifier with parallel feedback ($G_G = 0$; $G_D = 0$) are presented in [4].

Once the equivalent noise parameters R_n^{I}, G_n^{I}, and $Y_{\mathrm{cor}}^{\mathrm{I}}$ are known, the noise figure can be obtained with (1) while the minimum noise figure can be calculated using (2).

III. Conclusion

The formulas presented here enable the designer of amplifiers with feedback and lossy matching circuits to calculate the noise figure of their active devices, but perhaps more important, weigh the impact of the individual circuit elements on noise relative to each other. Such a comparison will help to decide which circuit principle to use for a given transistor. The expressions may seem rather complicated, but in most practical cases can be reduced to acceptable approximations. This is especially the case when high-gain transistors are employed. Programmable calculators may be used to quickly arrive at results.

IV. Appendix

The equivalent noise voltage v_1^{I} and the equivalent noise current i_1^{I} at the input terminal of the two-port shown in Fig. 1(a) are given by

$$v_1^{\mathrm{I}} = \frac{1}{Y_{21} - Y_{FB}} [Y_{21} v_1 - Y_{FB} v_{FB} - i_D] \tag{A.1a}$$

$$i_1^{\mathrm{I}} = i_1 + i_G + (Y_G + Y_{FB} + Y_{11}) v_1^{\mathrm{I}} - (Y_{11} v_1 + Y_{FB} v_{FB}) \tag{A.1b}$$

where

- v_1^{I} equivalent noise voltage at input terminal of two-port of Fig. 1(a);
- i_1^{I} equivalent noise current at input terminal of two-port of Fig. 1(a);
- v_1 noise voltage source of active (embedded) two-port;
- i_1 noise current source of active (embedded) two-port;
- v_{FB} equivalent noise voltage of feedback admittance Y_{FB};
- i_G equivalent noise current of input circuit admittance Y_G;
- i_D equivalent noise current of output circuit admittance Y_D.

By substituting

$$i_1 = i_n + Y_{\mathrm{cor}} v_1 \tag{A.2}$$

which defines the noncorrelated (i_n) and the correlated portions ($Y_{\mathrm{cor}} v_1$) of the current i_1 into (A.1) the mean-square values of the total noise current i_1^{I} and the total noise voltage v_1^{I} can be obtained. They are

$$\overline{|v_1^{\mathrm{I}}|^2} = \frac{1}{|Y_{21} - Y_{FB}|^2} \left(|Y_{21}|^2 \overline{|v_1|^2} + |Y_{FB}|^2 \overline{|v_{FB}|^2} + \overline{|i_D|^2} \right) \tag{A.3a}$$

$$\begin{aligned} \overline{|i_1^{\mathrm{I}}|^2} = {} & \overline{|i_n|^2} \\ & + \overline{|i_G|^2} + \left| \frac{Y_{21}}{Y_{21} - Y_{FB}} (Y_G + Y_{FB} + Y_{11}) - (Y_{11} - Y_{\mathrm{cor}}) \right|^2 \overline{|v_1|^2} \\ & + \left| \frac{Y_{FB}}{Y_{21} - Y_{FB}} (Y_G + Y_{FB} + Y_{11}) + Y_{FB} \right|^2 \overline{|v_{FB}|^2} \\ & + \left| \frac{Y_G + Y_{FB} + Y_{11}}{Y_{21} - Y_{FB}} \right|^2 \overline{|i_D|^2}. \end{aligned} \tag{A.3b}$$

In addition, the correlation between noise voltage v_1^{I} and noise current i_1^{I} can be expressed by the product

$$\begin{aligned} \overline{i_1^{\mathrm{I}} (v_1^{\mathrm{I}})^*} = {} & (Y_G + Y_{FB} + Y_{11}) \overline{|v_1^{\mathrm{I}}|^2} \\ & - (Y_{11} - Y_{\mathrm{cor}}) \left(\frac{Y_{21}}{Y_{21} - Y_{FB}} \right)^* \overline{|v_1|^2} \\ & - Y_{FB} \left(\frac{Y_{FB}}{Y_{21} - Y_{FB}} \right)^* \overline{|v_{FB}|^2} \end{aligned} \tag{A.3c}$$

with the help of the well-known Nyquist formulae

$$\overline{|v_1|^2} = 4KT_0 \Delta f R_n \tag{A.4a}$$

$$\overline{|v_{FB}|^2} = 4KT_0 \Delta f R_{FB} \tag{A.4b}$$

$$\overline{|i_D|^2} = 4KT_0 \Delta f G_D. \tag{A.4c}$$

We can now express the equivalent noise quantities of the overall network R_n^{I}, G_n^{I}, and $Y_{\mathrm{cor}}^{\mathrm{I}}$ of Fig. 1(c) in terms of the quantities R_n, G_n, and Y_{cor} of the embedded two-port and the admittances Y_G, Y_{FB}, and Y_D of Fig. 1(a). The results are presented as (4) in Section II.

Acknowledgment

The author would like to thank P. Hutchison for typing the formulae.

References

[1] J. Obregon, Y. LeTron, R. Funk, and S. Barvet, "Decade bandwidth FET functions," in *1981 Int. Microwave Symp. Dig. Tech. Pap.*, pp. 141–142.

[2] K. Honjo and Y. Takayama, "GaAs FET ultrabroad-band amplifiers for Gbit/s data rate systems," *IEEE Trans., Microwave Theory Tech.*, vol. MTT-29, pp. 629–636, July 1981.

[3] K. B. Niclas, W. T. Wilser, R. B. Gold, and W. R. Hitchens, "The matched feedback amplifier: Ultrawide-band microwave amplification with GaAs MESFET's," *IEEE Trans. Microwave Theory Tech.*, vol. MTT-29, pp. 285–294, Apr. 1980.

[4] K. B. Niclas, "Noise in broadband GaAs MESFET amplifiers with parallel feedback," *IEEE Trans. Microwave Theory Tech.*, vol. MTT-29, pp. 63–70, Jan. 1982.

[5] K. B. Niclas and R. R. Pereira, "Performance characteristics of lossy match versus feedback amplifiers in *S-C* band," in *Int. Solid State Circuit Conf. Dig. Tech. Pap.*, Feb. 1982.
[6] L. Besser, "Stability considerations of low-noise transistor amplifiers with simultaneous noise and power match," in *1975 Int. Microwave Symp. Dig. Tech. Pap.*, pp. 327–329.
[7] G. Vendelin, "Feedback effects on the noise performance of GaAs MESFET's," in *1975 Int. Microwave Symp. Dig. Tech. Pap.*, pp. 324–326.
[8] K. Hartmann and M. J. O. Strutt, "Changes of the four noise parameters due to general changes of linear two-port circuits," *IEEE Trans. Electron Devices*, vol. ED-20, pp. 874–877, Oct. 1973.
[9] S. Iversen, "The effect on feedback on noise figure," in *Proc. IEEE*, vol. 63, pp. 540–542, Mar. 1975.
[10] H. Rothe and W. Dahlke, "Theory of noisy fourpoles," in *Proc. IRE*, vol. 44, pp. 811–818, June 1956.
[11] H. A. Haus, *et al.*, "Representation of noise in linear two-ports," in *Proc. IRE*, vol. 48, pp. 69–74, Jan. 1960.

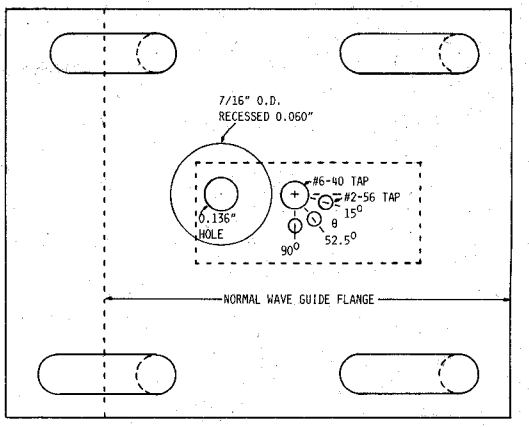

Fig. 1. Details of back plate with lateral adjustability.

Back Plate Mounted *X*-Band Lumped Element Gunn Oscillator[1]

ALEXANDER B. BERESKIN, FELLOW, IEEE

***Abstract*—A lumped *X*-Band Gunn oscillator, mounted on the waveguide back plate, provides full power output and tunability with provisions for altering the coupling to the waveguide in steps and/or continuously.**

Oscillator load variations can generally be expected to change both the frequency and amplitude of oscillation. In a cavity oscillator, a degree of control is obtained by interposing an iris between the cavity and the waveguide, thereby reducing the coupling between the oscillator and the load. Tuning screws, protruding into the cavity, can be used to adjust the frequency of oscillation.

The lumped element oscillator described in this paper does not use a frequency determining cavity and, therefore, other means have been devised to control the frequency of oscillation and the coupling between the oscillator and the load. These means differ substantialy from other lumped constant oscillators that have been described previously [1]–[5].

Fig. 1 shows details of a waveguide back plate on which the Gunn diode oscillator is to be mounted. This back plate is to be attached to the flange of an *X*-band waveguide at the transmitting end. When the back plate is removed from the waveguide, all of the oscillator's parts, both front and back, are readily accessible. The centered position of the waveguide and its flange are shown with dashed lines. The slotted back plate mounting holes make it possible to displace the back plate laterally, relative to the waveguide, by approximately 0.40 in.

The oscillator itself is shown in Fig. 2 and consists of a Gunn diode held in place by a chuck in the #6-40 tapped hole and a hairpin loop formed by a bare #24 tinned copper wire. The loop has a right-angle bend directly above the center of the #2-56 tapped holes and terminates flush with the surface of the back plate but does not contact it. The chuck is made by tapering the thread at the end and drilling and slotting the tip of the #6-40 copper screw. Tunability is provided by means of the #2-56 screw which has a central hole drilled in it and is lined with teflon sleeving obtained from teflon insulated hookup wire. As the #2-56 screw is made to engage the end of the hairpin loop it forms a coaxial variable capacitor with which the oscillator frequency can be varied continuously from outside the RF system.

Manuscript received July 10, 1981; revised November 6, 1981.
The author is with the Electrical Engineering Department, University of Cincinnati, Cincinnati, OH 45221.
[1]Patent applied for.

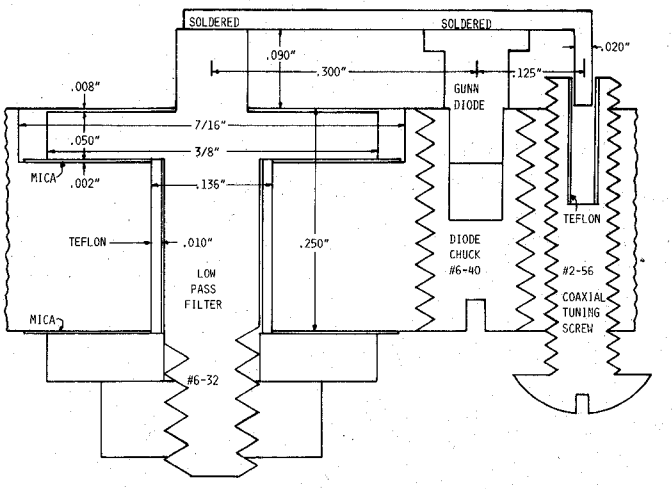

Fig. 2. Cross section of oscillator and low-pass filter ($\theta = 0°$).

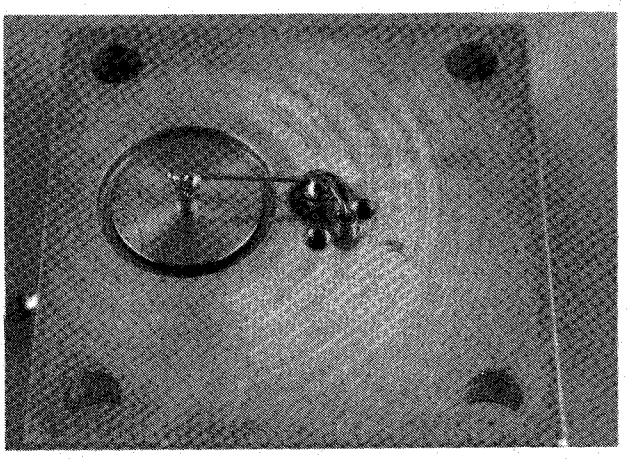

Fig. 3. Oscillator with coupling angle adjustability, $\theta = 52.5°$.

Fig. 3 is a photograph of the active side of an oscillator with

0018-9480/82/0500-0835$00.75 ©1982 IEEE